Applied Catalysis B: Environmental 115–116 (2012) 31–37

Contents lists available at SciVerse ScienceDirect

Applied Catalysis B: Environmental

journal homepage: www.elsevier.com/locate/apcatb

Semiconductor oxides-sensitized photodegradation of fenamiphos in leaching water under natural sunlight

José Fenoll [a,*], Pilar Hellín [a], Carmen María Martínez [a], Pilar Flores [a], Simón Navarro [b]

[a] Departamento de Calidad y Garantía Alimentaria, Instituto Murciano de Investigación y Desarrollo Agrario y Alimentario (IMIDA), C/Mayor s/n, La Alberca, 30150 Murcia, Spain
[b] Departamento de Química Agrícola, Geología y Edafología, Facultad de Química, Universidad de Murcia, Campus Universitario de Espinardo, 30100, Murcia, Spain

ARTICLE INFO

Article history:
Received 20 October 2011
Received in revised form
13 December 2011
Accepted 15 December 2011
Available online 23 December 2011

Keywords:
Water detoxification
Fenamiphos
Fenamiphos sulfoxide
Fenamiphos sulfone
Photocatalytic oxidation
Semiconductor materials

ABSTRACT

The photocatalytic degradation of fenamiphos in leaching water has been studied using zinc oxide (ZnO), different mixed-phase titanium dioxide (TiO_2), tungsten(VI) oxide (WO_3), and tin(IV) oxide (SnO_2) at pilot plant scale under natural sunlight. Photocatalytic experiments showed that the addition of semiconductors in tandem with the oxidant ($Na_2S_2O_8$) strongly enhances the degradation rate of fenamiphos in comparisons carried out with photolytic tests. The primary degradation of fenamiphos followed a pseudo-first order kinetics. The time required for 50% degradation was in the range 1–3 min for ZnO and TiO_2. The main photocatalytic intermediates (fenamiphos-sulfoxide and fenamiphos sulfone) detected during the degradation of fenamiphos were identified. Comparison of catalysts showed that ZnO is the most efficient for catalyzing the removal of fenamiphos and their metabolites. Thus, complete disappearance of all the compounds studied achieved after 240 min of illumination in the ZnO/$Na_2S_2O_8$ system.

1. Introduction

Fenamiphos (ethyl 4-methylthio-m-tolyl isopropylphosphoramidate), an organophosphorus pesticide, is primarily used to control nematodes in a wide range of horticultural crops and in turf. This systemic nematicide is an inhibitor of acetylcholinesterase. Fenamiphos quickly oxidizes to fenamiphos sulfoxide, which in turn, slowly oxidizes to fenamiphos sulfone [1]. The molecular structures of these chemicals are illustrated in Fig. 1. Due to their high solubility, fenamiphos and their metabolites may leach through the soil profile. Thus, residues of these compounds were found in surface and groundwaters [2,3]. Similar to fenamiphos, their metabolites are of a potential concern with regards to their fate and toxicity to water bodies. Consequently, it is of primary importance to apply remediation strategies to polluted waters or leachates in order to protect water resources. Advanced oxidation processes (AOPs), like H_2O_2/UV, O_3/UV and H_2O_2/O_3/UV, heterogeneous photocatalysis, homogeneous photo-Fenton, etc., have been proposed for treatment of polluted water by pesticides [4].

In particular, heterogeneous photocatalysis is an efficient technique to eliminate organic pollutants in water [5,6]. Semiconductors (TiO_2, ZnO, Fe_2O_3, ZnS, etc.) can act as sensitizers for light induced redox processes due to their electronic structure which is characterized by a filled valence band and an empty conduction band. This technique is based on the irradiation of semiconductor particles, usually titanium dioxide (TiO_2) because of its relatively high activity, its stability under operation conditions and its low cost [7]. Among the three main TiO_2 crystallographic forms (anatase, rutile and brookite), anatase and rutile forms have been investigated extensively as photocatalysts. Rutile generally exhibits lower catalytic activity than anatase [8]. The photocatalytic activity of TiO_2 is dependent on surface and structural properties of semiconductor. The commercial photocatalyst titanium dioxide Degussa P25 has been widely used and it is considered as the standard photocatalyst [9]. Degussa P25 consists of anatase and rutile in an approximately 3:1 proportion and is obtained by hydrolysis of $TiCl_4$ in a hot flame with a relatively short residence time [10].

When TiO_2 is irradiated with photons with wavelengths energy $h\nu \geq E_g$ (band gap energy), electrons (e^-) are promoted to the conduction band, leaving a positive hole (h^+) in the valence band. Holes can react with hydroxyl groups on the surface of the semiconductor to produce strongly oxidizing $OH^\bullet$ radicals. The hydroxyl radicals are extremely reactive ($E^\circ = 2.8$ V), non-selective and readily attack pesticides. As a result, these organic contaminants are sequentially transformed to simpler organic molecules that are eventually mineralized to CO_2, H_2O and inorganic salts [11]. On the other hand, electrons are trapped at surface sites and removed by reactions with adsorbed molecular O_2 to form superoxide anion radical $O_2^{\bullet -}$. Similar oxidation pathways to those of TiO_2 are confirmed in

* Corresponding author. Tel.: +34 968366798; fax: +34 968366792.
E-mail address: jose.fenoll@carm.es (J. Fenoll).

0926-3373/$ – see front matter © 2011 Elsevier B.V. All rights reserved.
doi:10.1016/j.apcatb.2011.12.023

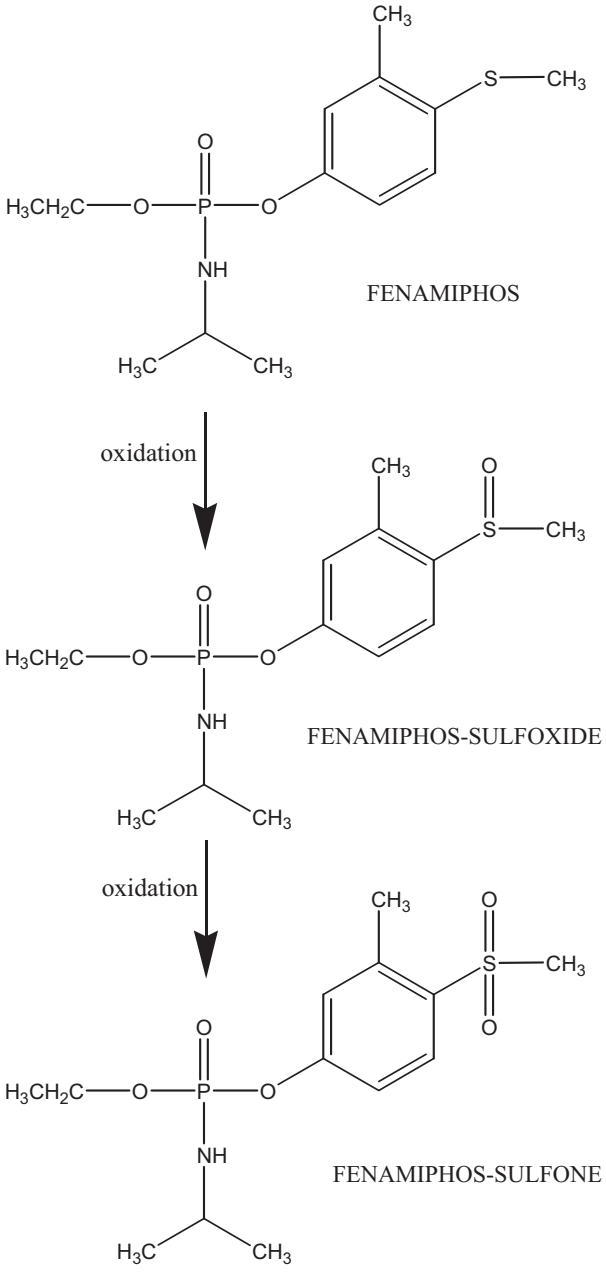

Fig. 1. Scheme for fenamiphos oxidation.

ZnO photocatalyst. ZnO is reported to be as reactive as TiO_2 under concentrated sunlight, since the band gap energy of ZnO is equal to that of TiO_2, i.e., 3.2 eV. No significant effort has been made in evaluating the photocatalytic efficiency of ZnO and TiO_2 on fenamiphos's oxidation. For this reason, in this study, the photocatalytic degradation of fenamiphos and their two main metabolites in leaching water has been investigated using zinc oxide (ZnO) and different mixed-phase titanium dioxide (TiO_2) as catalysts.

2. Experimental

2.1. Pesticides, metabolites and reagents

Fenamiphos, fenamiphos-sulfoxide, fenamiphos-sulfone were purchased from Dr. Ehrenstorfer (Augsburg, Germany): The commercial formulation used (NEMACUR 40 LE, fenamiphos 40%) was purchased from Fitodolores SL (Murcia, Spain). Zinc oxide (99.9%, $10\,m^2\,g^{-1}$, <70 μm), titanium dioxide anatase (99.9%, $45\,m^2\,g^{-1}$, 32 nm) and tungsten(VI) oxide (99.8%, powder <20 μm) were purchased from Alfa Aesar (Karlsruhe, Germany). Titanium dioxide mixture of rutile and anatase (99.5%, <100 nm) and tin(IV) oxide (99.9%, powder <44 μm) were supplied from Sigma–Aldrich Química S.A. (Madrid, Spain). Titanium dioxide P25 Degussa (99.5%, $50\,m^2\,g^{-1}$, <21 nm) was supplied from Nippon Aerosil Co Ltd. (Osaka, Japan). The titanium dioxide solid phases were characterized by means of powder X-ray diffractometry (XRD), on a Philips PW 1700. The samples were measured at 40 kV and 24 mA using Cu-Kα radiation at a scanning speed of 1° (2θ). The diffractogram of the X-ray of TiO_2 types are given in Fig. 2. The contents of anatase (A) and rutile (R) phases in the powders were 70A:30R for TiO_2 P25 Degussa, 25A:75R for TiO_2 mixture of rutile:anatase and 90A:10R for TiO_2 anatase. Sodium peroxydisulfate (98%) was purchased from Panreac Química (Barcelone, Spain). Acetonitrile was supplied by Scharlau (Barcelone, Spain).

2.2. Preparation of solutions

Stocks solutions ($1000\,\mu g\,mL^{-1}$) of each pesticide standard were prepared in acetonitrile, protected from light and stored at 5 °C. A pesticide intermediate standard solution was prepared by dilution in the same solvent to obtain a concentration of $10\,\mu g\,mL^{-1}$. Several standard solutions, with concentrations of 0.5–200 $\mu g\,L^{-1}$, were injected to obtain the linearity of detector response.

2.3. Leaching experiment

The soil selected for the study was taken from Campo de Cartagena (Murcia, SE Spain), air dried, ground, sieved through 2 mm mesh sieve and stored at 4 °C. The characteristics of the soil were as follows: pH 8.70; organic matter content 0.22%, electrical conductivity $3.54\,dS\,m^{-1}$ and clay loam texture (33% clay, 30% silt, 37% sand).

All experiments were performed according to the OECD guidelines [12]. Downward movement of the fungicides was studied in polyvinyl chloride (PVC) columns of 30 cm (length) × 4 cm (i.d.) packed with 200 g of soil (bulk density, $1.34\,g\,cm^{-3}$). The top 3 cm of the columns were filled with sea sand and the bottom 3 cm with sea sand plus nylon mesh with an effective pore diameter of 60 μm to minimize the dead-end volume and prevent losses of soil during the experiment. Before the application of the compound, the columns were conditioned with 0.01 M $CaCl_2$ in distilled water to their maximal water holding capacity and then allowed to drain for 24 h. The pore volume (PV) of the packed columns was estimated by the weight difference of water-saturated columns versus dry columns. The calculated PV of the soil columns after saturation was 66 ± 3 mL. Afterwards, 2 mL of a methanol/water solution (10/90, v/v) containing 25 μg of fenamiphos were added to the top of each column. Twenty-four hours after pesticide application (when solvent was completely evaporated), the compounds were leached using a peristaltic pump with 0.01 M $CaCl_2$ at a rate of $50\,mL\,day^{-1}$ (equivalent to 21 mm) for 22 days. $CaCl_2$ instead of water was used in order to minimize soil mineral balance disruption. After this time, the columns were opened and the soil was separated into two segments of approximately 10 cm each. Five replications were run at room temperature (21 ± 2 °C), avoiding direct light.

2.4. Solar photocatalysis experiment

The water used in the photodegradation studies was obtained from 8 lysimeters (3.5 m × 4 m × 1 m) from an experimental greenhouse located in Campo de Cartagena (SE Spain). A clay loam soil (pH 8.7 and OM = 0.22%) was used. The soil was irrigated every four days by three dripperlines (45 min/day and

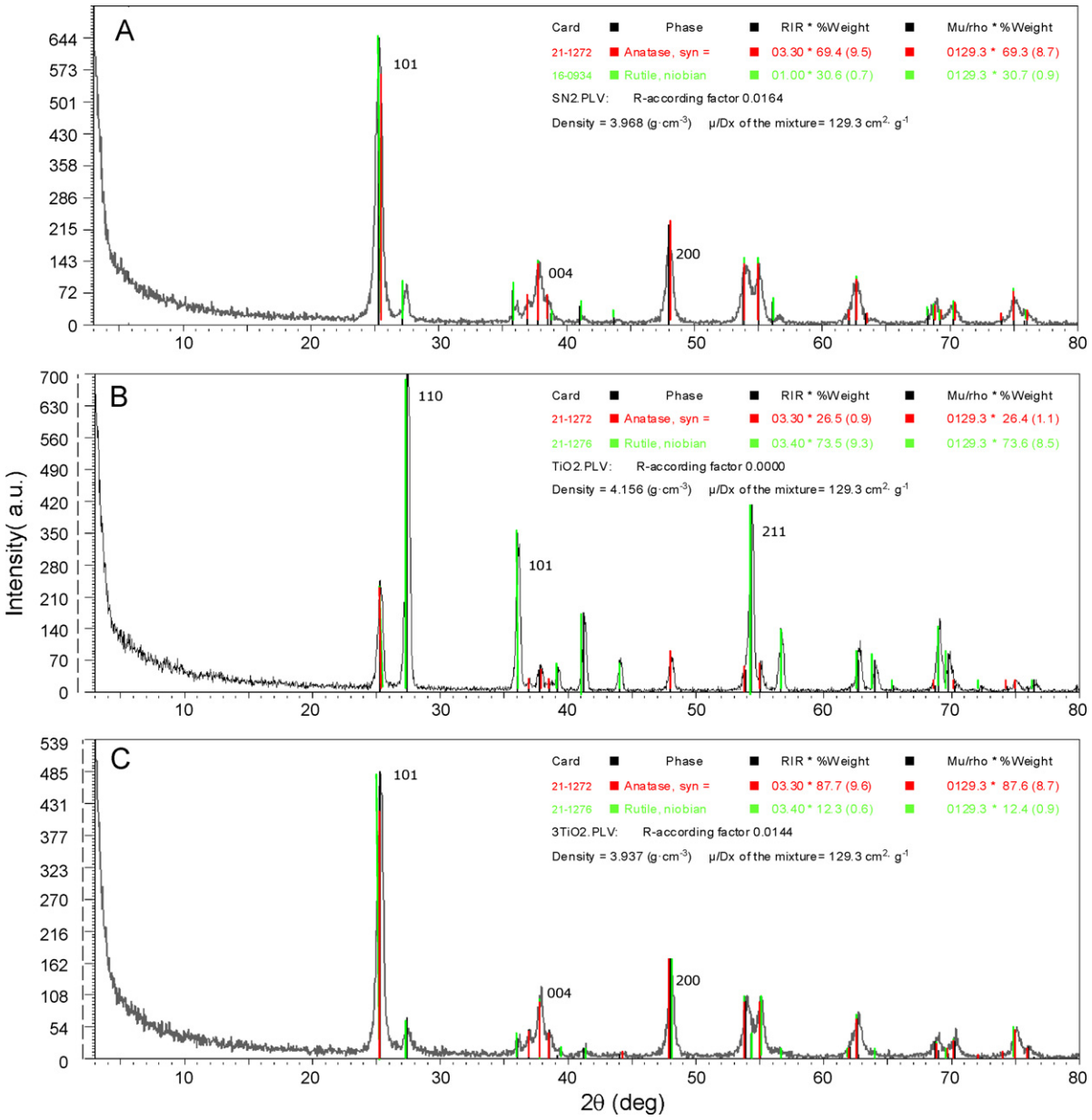

Fig. 2. XRD patterns of (A) TiO_2 P25 Degussa, (B) TiO_2 anatase:rutile (1:3) and (C) TiO_2 anatase ((▬) anatase, (▬) rutile).

50 mL min^{-1} per emitter). About 8 L day^{-1} were collected from each lysimeter. The water had pH 8.41, EC = 4.32 dS m^{-1}, TOC = 130 mg L^{-1}, NO_3^- = 547 mg L^{-1}, and NO_2^- = 0.12 mg L^{-1}. The leaching water (1000 L) was collected and transported to the storage tank. Finally, the water was spiked with commercial product and stored in dark at ambient temperature for one week.

The experiment was carried out in a pilot plant in Murcia, SE Spain (latitude 37°59′ N, longitude 1°08′ W) using natural sunlight irradiation during July 2010. The values (mean ± SD) of visible plus near infrared (400–1100 nm), UVA (315–400 nm), UVB (280–315 nm), and UVC (200–280) radiation were measured with a portable photoradiometer Delta Ohm HD 2102.2 (Caseelle di Selvazzano, Italy). Fig. 3 shows the mean values (n = 15) recorded from UV radiation during the sampling.

The solar pilot plant used in this experiment is based on compound parabolic collector (CPC) technology [13]. This small prototype consists of one photoreactor module (1.27 m^2) with five borosilicate tubes (200 cm length × 4 cm i.d.) mounted on a curved polished aluminum reflectors (0.9 cm radius of curvature) running in the east-west. The water flows directly from one to another tube connected in series and finally to the reservoir tank (250 L) and a centrifugal pump (0.55 kW) then returns the water (45 L min^{-1}) to the collector tubes in a closed circuit. The reaction system was continuously stirred to achieve a homogeneous suspension and thermostated by circulating water to keep the temperature at 25 ± 2 °C. The illuminated volume was 12.6 L and the dead volume of PVC tubes about 6.5 L. Storage tank, flowmeter, sensors (pH, O_2 and T), pipes, and fittings complete the installation.

At the beginning of the assay, the leaching water (150 L) was mixed with commercial product (NEMACUR 40 LE, Aragonesas) to reach a spiking level of about 0.1 mg L^{-1} of fenamiphos, homogenizing the mixture for 20 min to constant concentration in the dark with collectors covered by a black awning. Finally, the photosensitizer (100 mg L^{-1}) and oxidant (100 mg L^{-1} of $Na_2S_2O_8$ for ZnO and 150 mg L^{-1} for TiO_2, WO_3 and SnO_2) were added and the cover removed after 15 min. Samples were collected at 0, 5, 10, 20, 45,

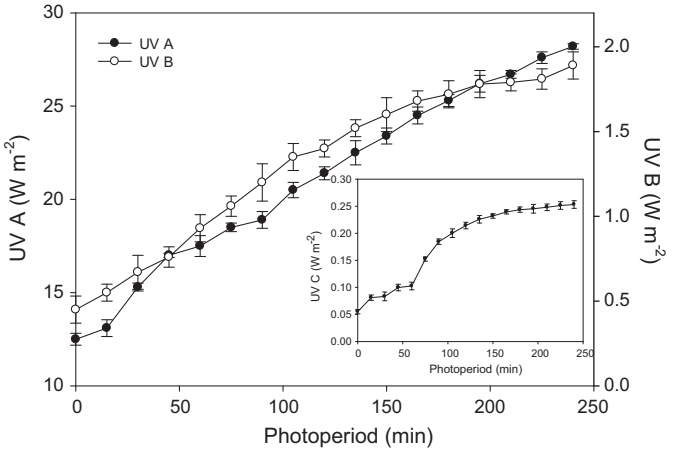

Fig. 3. Mean values ($n = 15$) for UV-A and UV-B radiation recorded in the different sample points of the photoperiod. Insert graphic shows UV-C radiation. Error bars denote standard deviation.

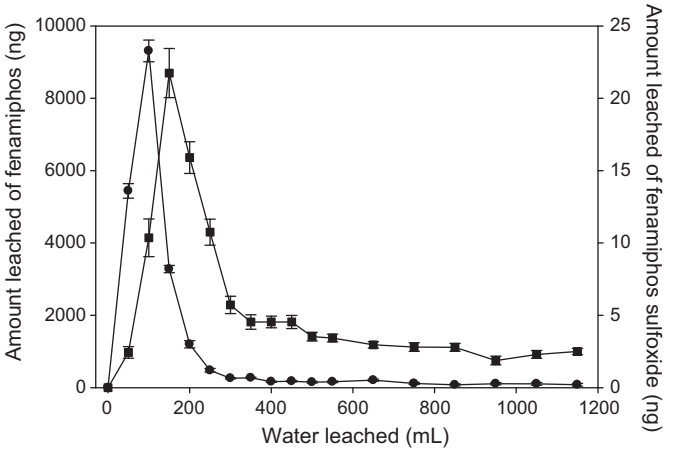

Fig. 4. Relative breakthrough curves (BTCs) of fenamiphos (●) applied to soil columns and fenamiphos sulfoxide (■) detected in leachates.

60, 120 and 240 min between 10 a.m. and 2 p.m. Periodically, air was injected into the tank. A parallel blank assay without catalyst and $Na_2S_2O_8$ (photolysis experiment) was run. In both cases, assays were replicated three times.

2.5. Analytical determinations

Water samples were extracted and analyzed according to the procedure described by Fenoll et al. [14]. The separation, identification and quantification of the selected pesticides were carried out using an HPLC system (consisting of vacuum degasser, autosampler and a binary pump) (Agilent Series 1100, Agilent Technologies, Santa Clara, CA, USA) equipped with a reversed phase C8 analytical column of 150 mm × 4.6 mm and 5 μm particle size (Zorbax Eclipse XDB-C8) and an G6410A triple quadrupole mass spectrometer from Agilent equipped with an ESI interface operating in positive ion mode.

Blank samples were used to establish the limit of detection (LOD) and the limit of quantification (LOQ). Both, LODs and LOQs were calculated from the signal-to-noise (S/N) ratio 3 and 10, respectively. The calibration samples were analyzed by spiking pesticides at 0.5–200 $\mu g\,L^{-1}$ levels into water samples in five replicates. The correlation coefficient was found to be >0.99 and the limits of quantification were in the range 0.01–0.02 $\mu g\,L^{-1}$ for fenamiphos sulfone and fenamiphos, respectively. To test the repeatability of the method ten water samples were spiked at two concentration levels (10 $\mu g\,L^{-1}$ and 50 $\mu g\,L^{-1}$). In order to evaluate the accuracy of the method, the recoveries were determined by the standard addition technique.

2.6. Statistical analysis

The curve fitting and statistical data were obtained using SigmaPlot version 12.0 statistical software (Systat, Software Inc., San Jose, CA).

3. Results and discussion

3.1. Preliminary studies

The breakthrough curves (BTCs) obtained from the preliminary leaching study allowed classifying fenamiphos as a "leacher" compounds since 48% and of the initial amount applied to the soil was found in the leachates (Fig. 4). Fenamiphos was rapidly oxidized to fenamiphos sulfoxide which was also found in the leachates after the addition of the first 50 mL. On the contrary, fenamiphos sulfoxide was not further oxidized to fenamiphos-sulfone and its product was not found in the soil or in the leachates probably due to the low soil organic matter content.

3.2. Effect of different semiconductors

Metal oxides and sulfides represent a large class of semiconductor materials suitable for photocatalytic purposes. Compared with the other semiconductors, the use of ZnO and TiO_2 strongly enhanced the photodecomposition of fenamiphos, and more than 99% of the pesticide initially present in the leaching water being degraded after 10 min of illumination (Table 1). However, in the presence of the other semiconductors, the remaining mean percentages after 10 min of irradiation were 59% and 68% for SnO_2 and WO_3, respectively.

The band gap of ZnO and TiO_2 is ca. 3.2 eV, which corresponds to radiation wavelength around 390 nm. The observed low activity of WO_3 in comparison with these semiconductors can be related to it smaller band gap (2.8 eV) since its positive conduction band level (around 0.37 vs NHE) might limit its use as a photocatalyst in terms of the oxidative degradation of organic compounds [7]. On the other hand, although SnO_2 has higher band gap than ZnO and TiO_2 (3.9 eV), the lower activity in this case can be attributed to the significantly lower wavelength (318 nm) necessary to activate the catalyst.

3.3. Effect of ZnO and $Na_2S_2O_8$ concentrations

In slurry photocatalytic processes, the amount of photocatalyst and oxidant are two important parameters that can affect the degradation rates of the pesticides. The influence of the photocatalyst concentration on the disappearance kinetics of fenamiphos has been investigated employing different concentrations of ZnO

Table 1
Photocatalytic activity of different semiconductor oxides as catalyst loading after 10 min of illumination.

Semiconductor	% Degradation
Photolysis	7.3
ZnO	99.9
TiO_2 P25 Degussa	99.9
TiO_2 anatase	99.7
TiO_2 anatase:rutile (1:3)	99.4
WO_3	68.0
SnO_2	59.1

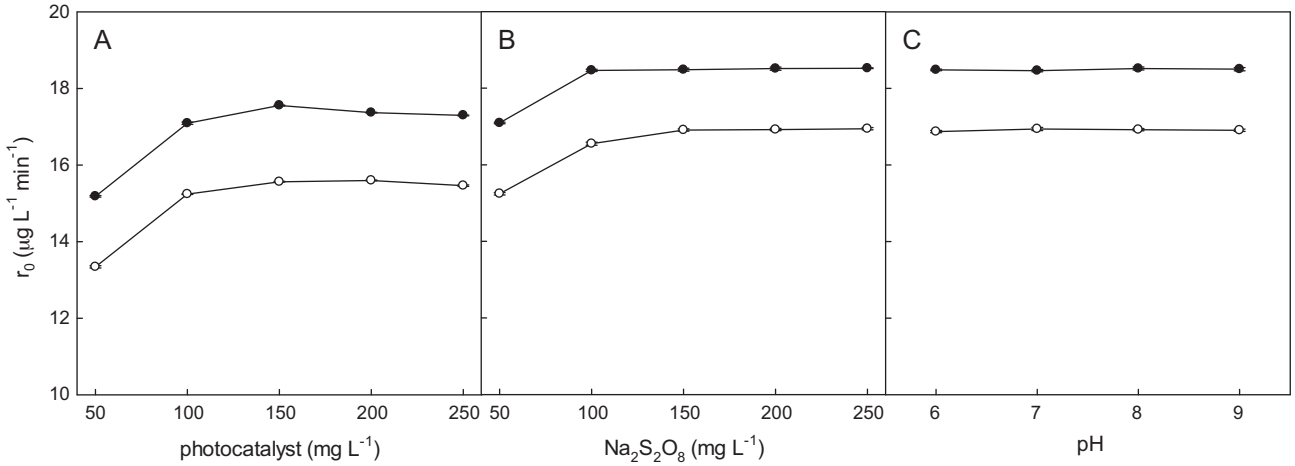

Fig. 5. Optimization of photocatalytic heterogeneous process with ZnO (●) and TiO_2 (○) after 10 min of illumination. (A) photacatalyst concentration (fixed [$Na_2S_2O_8$ = 50 mg L^{-1}], pH_0 8.2), (B) $Na_2S_2O_8$ concentration (fixed [photocatalyst = 100 mg L^{-1}], pH_0 8.2) and (C) initial pH (fixed [ZnO/$Na_2S_2O_8$ = 100 mg L^{-1}/100 mg L^{-1}] and [TiO_2/$Na_2S_2O_8$ = 100 mg L^{-1}/150 mg L^{-1}]).

and TiO_2 from 50 to 250 mg L^{-1}. The reaction rate is directly proportional to the mass of catalyst. However, above a certain value the reaction rate levels off and becomes independent of the concentration the catalyst. According to Hermann [15], this limit depends on the geometry and the working conditions of the photoreactor. This plateau fits with to the maximum amount of catalyst in which all the particles are totally illuminated, after this limit a screening effect excess particle occurs. In this study, significant differences were observed in the reaction rate when the concentration of the catalyst was increases from 0 to 100 mg L^{-1} for ZnO and TiO_2 and the optimum value for ZnO and TiO_2 was 100 mg L^{-1} (Fig. 5A).

The electron–hole recombination is one of the main drawbacks in the application of semiconductor photocatalysis as it causes waste of energy. In the absence of suitable electron acceptor, recombination step is predominant, and thus, it limits the quantum yield. The addition of an electron acceptor, such as hydrogen peroxide (H_2O_2), potassium bromate ($KBrO_3$), or inorganic peroxide ($S_2O_8^{2-}$), to a semiconductor suspension usually enhances the photodegradation rate of organic pollutants, since these substances capture the photogenerated electrons more efficiently than dissolved oxygen, leading to a reduction of the electron–hole recombination [8]. $Na_2S_2O_8$ traps the photogenerated electron and reduces the probability of recombination with the positive hole, generating $SO_4^{\bullet-}$ radicals, which are also a very strong oxidizing species (reduction potential of $SO_4^{\bullet-}$ E° = 2.6 V), and more hydroxyl radicals. In order to examine the role of peroxydisulfate, experiments of the photocatalytic degradation of fenamiphos employing different initial concentrations of the oxidant were conducted. In the illuminated ZnO and TiO_2 suspension, complete degradation (>99.5%) of fenamiphos occurred after 10 min using the tandem ZnO/$Na_2S_2O_8$ (100 mg L^{-1} of each one) and TiO_2/$Na_2S_2O_8$ (100/150 mg L^{-1}) (Fig. 5B).

3.4. Effect to dissolved oxygen, pH and temperature

One practical problem in using photosensitizers is e^-/h^+ recombination, which can be reduced in the presence of a suitable electron acceptor. For this purpose, air was introduced in the tank at regular intervals to maintain the O_2 concentration around 5–6 mg L^{-1}. Molecular oxygen plays an important role in the photooxidation process. The principal role of dissolved oxygen in the photodegradation process is to act as an electron sink, although some authors suggest that it can act as "inner filter" or "scavenger" because molecular oxygen has absorption bands at 185 and 254 nm [16]. In addition, oxygen also participates in the reaction to produce oxyl and peroxyl radicals. However, the spectrum sunlight at earth's surface begins around 300 nm. Therefore, the filter effect was not important in our case.

According to previous studies, pH of the solution appears to play an important role in the photocatalytic process of various pollutants because it influences the surface charge of the semiconductor, thereby affecting interfacial electron transfer and the photoredox process. The influence of the initial pH value on the initial photodegradation rate of fenamiphos for the ZnO and TiO_2 suspensions was studied. No significant differences were observed in the reaction rate when the pH was increases from 6 to 9 for ZnO and TiO_2 (Fig. 5C). In the present case, the experiments were carried out at an initial pH of around 8.2. As photodegradation progressed, there was a weak decrease in pH (about 0.3–0.4 units). At acidic pH, ZnO can react with acids to produce the corresponding salt and at alkali pH, it can react with a base to form $Zn(OH)_2$. Consequently, the toxicity in the illuminated ZnO system can be magnified by the increase of Zn^{2+} in the solution. We observed a weak increase in the concentration of Zn^{2+} during the degradation process (from 0.12 mg L^{-1} to 3.21 mg L^{-1} after 240 min). The measurements made of Zn^{2+} by ICP during the illumination time confirm the dissolution and photodissolution of ZnO, especially during the first 30 min. As precipitation of the insoluble hydroxide salt is the most common form of treatment the pH of the water was adjusted to about 9.5 to form the precipitate. Thus, the concentration of Zn^{2+} in water after treatment was below 0.1 mg L^{-1}. Metal removal is not complete until the metal solid is physically removed from the water, by subsequent sedimentation and filtration.

Regards temperature, photocatalytic systems do not require heating and operate at room temperature because of photonic activation and, in our study, temperature was maintained at 25 ± 2 °C.

3.5. Kinetics of photo-assisted catalysis in ZnO and TiO_2 suspensions

Kinetics of fenamiphos degradation was calculated using the first-order equation:

$$r = \frac{-dC}{dt} = k'C$$

$$C_t = C_0 e^{-k't} \text{ or } \ln\frac{C_0}{C_t} = k't$$

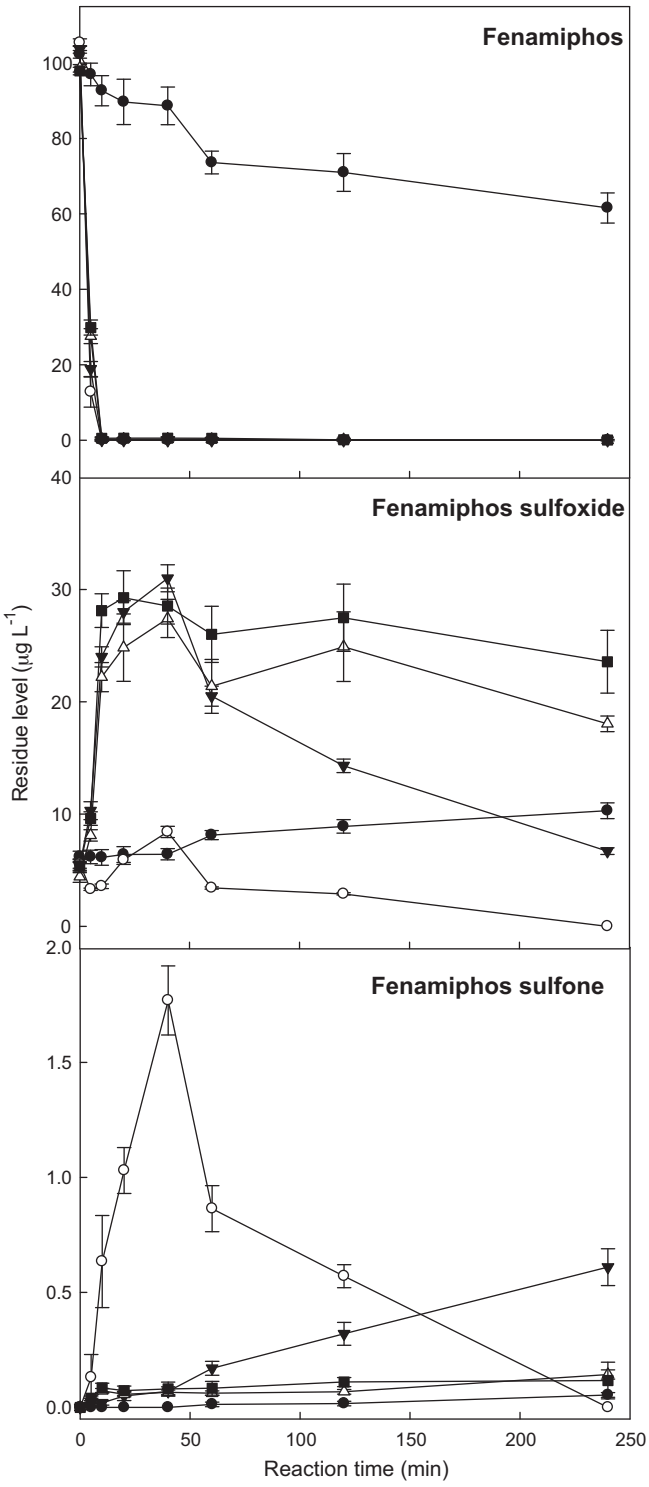

Fig. 6. Degradation kinetics of fenamiphos and quantitative analysis of derivatives detected in water by photolysis (●), and heterogeneous photocatalysis with ZnO (○), TiO_2 P25 Degussa (▼), TiO_2 anatase:rutile (1:3) (■) and TiO_2 anatase (△) during the photoperiod.

where r is the mineralization rate of the pesticide, C_0 and C_t are the pesticide concentration at times zero and t, respectively, and k' (in units of time^{-1}) is the apparent first-order rate constant.

The photocatalytic degradation of fenamiphos in the presence or in the absence of the four catalysts (ZnO, TiO_2 P25 Degussa, TiO_2 anatase and TiO_2 anatase:rutile (1:3) is represented in Fig. 6. In the presence of ZnO and TiO_2 P25 Degussa complete disappearance was achieved after 20 min and 40 min of illumination, respectively. The residual levels of fenamiphos after 40 min in the presence of TiO_2 anatase and TiO_2 anatase:rutile (1:3) was 0.3 and 0.6 μg L^{-1}, respectively. No significant differences were observed in the reaction rate when ZnO or TiO_2 were used. However, ZnO appears to be more effective than TiO_2 for the fenamifos-sulfoxide and fenamifos-sulfone oxidation since, in the ZnO system, complete disappearance of fenamifos-sulfoxide and fenamifos-sulfone were achieved after 240 min of illumination. The observed differences are certainly related to the structure, diameter of particles and electrical properties of the photocatalyst [17]. Thus, its non-stoichiometry leads to electron mobility of at least two orders of magnitude higher than TiO_2. This results in a quicker charge transfer with the various species in the solution and consequently to lower recombination rates in comparison to TiO_2 [18]. Comparison of the three TiO_2 catalysts showed that P25 Degussa is the most efficient for catalyzing the removal of fenamifos-sulfoxide. In all TiO_2 cases, residues of fenamifos-sulfoxide and fenamifos-sulfone were found after the irradiation time. The residual levels of fenamifos-sulfoxide at the end of the experiment (240 min) ranged from 6.7 to 25.6 μg L^{-1} for TiO_2 P25 Degussa and TiO_2 anatase:rutile (1:3), respectively. Fenamifos-sulfoxide residue at the end of the experiment was higher for TiO_2 P25 Degussa that for TiO_2 anatase and TiO_2 anatase:rutile (1:3) due to increased photoxidation rate of fenamifos sulfoxide when P25 Degussa was used. The higher photoactivity of TiO_2 P25 Degussa has been attributed to its crystalline composition of rutile and anatase. It was postulated that the smaller band gap of rutile absorbs the photons and generates electro–holes pairs. Then the electron transfer takes place from the rutile conduction band to electron traps in the anatase phase. This process inhibits the recombination and allows the hole to move to the surface of the particle to react [19].

Table 2
Kinetic parameters for photocatalysis (ZnO and TiO_2) of fenamiphos in leaching water under natural sunlight.

Semiconductor	$C_t = C_0 e^{-k't}$	R^2	$S_{y/x}$[a]	$t_{½}$ (min)
ZnO	$C_t = 105.4e^{-0.427t}$	0.999	0.61	1.6
TiO_2 P25 Degussa	$C_t = 103.7e^{-0.352t}$	0.999	1.30	2.0
TiO_2 anatase	$C_t = 99.0e^{-0.278t}$	0.994	2.68	2.5
TiO_2 anatase:rutile (1:3)	$C_t = 98.4e^{-0.263t}$	0.992	3.06	2.6

[a] Standard deviation of the fitting (standard error of estimate).

In the absence of a catalyst, the photolytic decomposition of fenamiphos occurred at a lower rate than that observed in the photocatalysis process, and only a 40% reduction of its initial concentration was achieved after 240 min of light exposure.

The kinetic parameters of fenamiphos are shown in Table 2 where the apparent rate constants and half-lives are listed. In all cases, the kinetics of dissipation (Fig. 6) followed an apparent first-order degradation curve, with R^2 ranging from 0.993 to 0.999 and standard error of the estimate lower than 3.1 in the most unfavorable case. The half-lives for fenamiphos in the presence of ZnO and TiO_2 were about 1–3 min.

4. Conclusions

The photooxidation of fenamiphos has been investigated using different semiconductor materials under natural sunlight. The photoxidation of this pesticide followed first order kinetics and parameters like the concentration of the catalyst and oxidant played an important role affecting the reaction rate. ZnO proved to be the more efficient photocatalyst since the oxidation and decomposition of fenamiphos proceeded at higher reaction rates. Thus, complete disappearance of fenamiphos sulfoxide and fenamiphos sulfone was achieved only in the presence of ZnO. In general, the

efficiency of the catalysts in the photooxidation of fenamifos and their metabolites was in the order: ZnO > TiO_2 P25 Degussa > TiO_2 anatase ≈ TiO_2 anatase:rutile (1:3). Heterogeneous photocatalytic processes, especially those involving ZnO photocatalysis, offers a rapid and economical technology for surface and groundwater remediation, especially in Mediterranean areas like SE Spain which receive more than 3000 h of sunlight per year.

Acknowledgments

The authors are grateful to Inmaculada Garrido and María V. Molina for technical assistance and to FEDER and European Social Funds and the Ministerio de España de Ciencia e Innovación through the Ramón and Cajal Subprogram and the project AGL2010-20458-C02-01 for the financial support.

References

[1] T. Roberts, D. Hutson, in: T. Roberts, D. Hutson (Eds.), Part One: Herbicides and Plant Growth Regulators, The Royal Society of Chemistry, Cambridge, UK, 1998.
[2] P. Franzmann, L. Zappia, A. Tilbury, B. Patterson, G. Davis, T. Mandelbaum, Bioremediation J. 4 (2000) 237–248.
[3] G. Patrick, A. Chiri, D. Randall, E.L. Libelo, R.D. Jones, Fenamiphos environmental risk assessment, US Environmental Protection Agency, Provided for SRRD by EFED's Fenamiphos RED Team, 2001, Available from: http://www.epa.gov/oppsrrd1/REDs/fenamiphos_ired.pdf.
[4] S. Navarro, J. Fenoll, N. Vela, E. Ruiz, G. Navarro, Chem. Eng. J. 167 (2011) 42–49.
[5] I.K. Konstantinou, T.A. Albanis, Appl. Catal. B: Environ. 42 (2003) 319–335.
[6] P. Pichat, S. Vannier, J. Dussaud, J.P. Rubis, Sol. Energy 77 (2004) 533–542.
[7] Y.F. Rao, W. Chu, Chem. Eng. J. 158 (2010) 181–187.
[8] S. Ahmed, M.G. Rasul, R. Brown, M.A. Hashib, J. Environ. Manage. 92 (2011) 311–330.
[9] N. Serpone, G. Sauve, R. Koch, H. Tahiri, P. Pichat, P. Piccinini, E. Pelizzetti, H. Hidaka, J. Photochem. Photobiol. A: Chem. 94 (1996) 191–203.
[10] T. Docters, J.M. Chovelon, J.M. Herrmann, J.P. Deloume, Appl. Catal. B: Environ. 50 (2004) 219–226.
[11] M.G. Antoniou, J.A. Shoemaker, A.A. De La Cruz, D.D. Dionysiou, Environ. Sci. Technol. 42 (2008) 8877–8883.
[12] OECD, Organisation for Economic Cooperation and Development Guidelines for Testing of Chemicals, N(312, Leaching in Soil Columns, Paris, 2007.
[13] S. Malato, J. Blanco, A. Vidal, C. Richter, Appl. Catal. B: Environ. 37 (2002) 1–15.
[14] J. Fenoll, P. Hellin, C.M. Martinez, P. Flores, S. Navarro, Talanta 85 (2011) 975–982.
[15] J.M. Herrmann, Top. Catal. 34 (2005) 49–65.
[16] H. Shirayama, Y. Tohezo, S. Taguchi, Water Res. 35 (2001) 1941–1950.
[17] N.H. Salah, M. Bouhelassa, S. Bekkouche, A. Boultif, Desalination 166 (2004) 347–354.
[18] V. Kitsiou, N. Filippidis, D. Mantzavinos, I. Pouios, Appl. Catal. B: Environ. 86 (2009) 27–35.
[19] D.C. Hurum, A.G. Agrios, K.A. Gray, T. Rajh, M.C. Thurnauer, J. Phys. Chem. B 107 (2003) 4545–4549.